Tin-free synthesis of a ternary random copolymer for BHJ solar cells: Direct (Hetero)Arylation *versus* Stille polymerization

G. Marzano,[a] D. Kotowski,[b] F. Babudri,[a] R. Musio,[a] A. Pellegrino,[c] S. Luzzati,[b] R. Po,[c]

G.M. Farinola[*a]

[a]Dipartimento di Chimica, Università degli Studi di Bari Aldo Moro, Via Orabona 4, 70125, Italy

Fax: +39-0805442064

E-mail: gianlucamaria.farinola@uniba.it

[b]Consiglio Nazionale delle Ricerche, CNR, Istituto per lo Studio delle Macromolecole, ISMAC, Milan, Italy

[c]Centro Ricerche per le Energie Rinnovabili e l'Ambiente – Istituto Eni Donegani, Eni SpA, Via Fauser 4, 28100 Novara, Italy

KEYWORDS. Random copolymers, conjugated polymers, direct arylation, cross-coupling, organic photovoltaics, BHJ solar cells.

ABSTRACT. In a recent report (*Eur. J. Org. Chem.* **2014**, *30*, 6583) we emphasized the importance to address research efforts in OPV active materials toward synthetic processes scalable up to industrial production. In this context, palladium-catalysed direct (hetero)arylation polymerization (DHAP) can be a suitable approach to reduce the number of reaction steps and to avoid the use of toxic reagents in the synthesis of donor polymers. Random donor-acceptor copolymers have been shown to be promising materials for bulk heterojunction solar cells (BHJ) with high efficiencies and increased thermal stability. We report here the synthesis by DHAP of a ternary double-acceptor/donor random copolymer including benzo[*c*][1,2,5]thiadiazole and benzo[*d*][1,2,3]triazole as the accepting units and benzo[1,2-*b*;4,5-*b'*]dithiophene as the donor moiety. The results are discussed in comparison with the synthesis of the same polymer via the Stille polymerization. The coupling products formed in the early stage of the polycondensation have been isolated and characterized by NMR spectroscopy to gain insight into the regiochemistry of DHAP. The polymers synthesized have been tested in bulk-heterojunction

solar cells with $PC_{71}BM$ as the electron acceptor material. Power conversion efficiencies (up to 2.8 %) are comparable or lower (depending on the processing conditions) than those of the same polymer synthesized *via* the Stille coupling reaction. However, the DHAP protocol is more convenient in terms of synthetic complexity.

Introduction. Semiconducting polymers are widely used in Organic Photovoltaics (OPVs) as light absorbing/electron donor materials in bulk hetero-junction (BHJ) solar cells.[1-2] The interest in polymer solar cells stems from the low-cost solution processability of organic polymers by conventional printing techniques and from the possibility of obtaining light weight, flexible and coloured modules. In the last few years, remarkable improvements in power conversion efficiencies (PCEs) of lab-scale BHJ devices were achieved (over 10%)[3-4] using copolymers with alternating electron-donor and electron-acceptor units (D-A copolymers), thus confirming the great potential of this technology. The D-A structural motif gives the possibility to tailor the HOMO-LUMO gap energy of the donor polymers by proper choice of the monomers involved in the polymerization process.[5]

However, scalability at industrial level of the synthesis of D-A polymers is still a major issue preventing large scale use of plastic solar cells.[1-2] In fact, most of the best performing copolymers are prepared by the Stille cross-coupling reaction, which involves the use of organo-stannanes. Besides being highly toxic, the stannylated monomers are synthesized *via* multistep organometallic processes and require demanding purification steps.[6-9]

In the recent literature, Direct (Hetero)Arylation Polymerization (DHAP) has been reported as a clean and cheap route to conjugated polymers compared to conventional organometallic cross-

coupling reactions.[10-17] It involves a halogenated (most commonly I, Br) aromatic monomer and an aromatic substrate bearing a C-H bond activated *via* a Pd-catalyst. The reaction typically requires the presence of a base, not only to neutralize the stoichiometric amount of the acid formed during the process, but also to assist the C-H bond activation step. The possibility of avoiding the use of organometallic reactants undoubtedly makes this approach particularly appealing for industrial scalability.[1] However, the possible formation of structural defects in the polymer backbone (*i.e.* homo-coupling, branching and cross-linking processes)[18] can negatively affect the electronic properties of the final materials and their performances in devices. In addition, the conditions of DHAP reactions need to be optimized for each different combination of reactants.

The present contribution describes our investigations on the potentialities and features of DHAP as a synthetic route to random ternary copolymers.

The random copolymer approach appears particularly promising[19] for the possibility of fine-tuning the opto-electronic properties and the solubility of the final materials by tailoring the chemical nature and the relative amount of the monomers involved in the polymerization. In addition, the random structure can positively affect the active layer stability, as observed in the case of low-regioregular poly(3-hexylthiophene)s (P3HTs).[20]

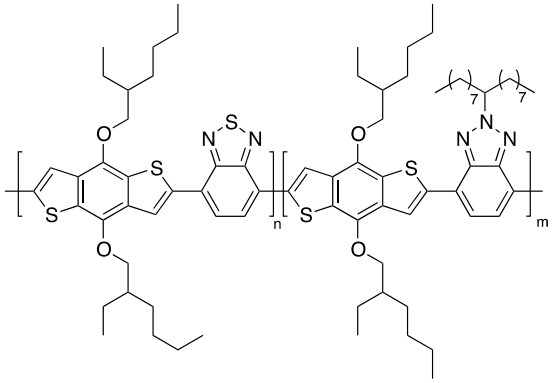

Figure 1. Repeating units of the random copolymer P

To the best of our knowledge, only one example of DHAP protocol applied to the synthesis of semi-random polymers involving three reacting units has been reported so far.[21] This study by Thompson et al. critically discussed the potentialities and drawbacks of DHAP of unsubstituted thiophene and 3-hexyl-2-bromothiophene as donor comonomers, and 4,7-bis bromobenzothiadiazole or dibromo-dithienyl-diketopyrrolopyrrole as accepting comonomer. Although this polymerization is in fact a three component reaction, the donor units of the polymer reported are all thiophene rings differing only for the alkyl substituents.

Here, we report a study on DHAP of three different monomers which affords a random ternary D-A copolymer **P** (Figure 1), with benzo[*c*][1,2,5]thiadiazole and benzo[*d*][1,2,3]triazole as the accepting units and benzo[1,2-*b*;4,5-*b'*]dithiophene as the donor moiety.

The same random copolymer **P** obtained via Stille coupling reaction was already reported[22] and we have carried out a comparative study on the properties of the materials obtained *via* the two different protocols, also covering the performances in solar cells. We have performed a detailed structural analysis by NMR spectroscopy of the main coupling products formed in the early stage of the direct arylation process to shed light on the regiochemical course of the reaction.

Copolymer **P**, synthesized *via* Stille cross-coupling, exhibited power conversion efficiency of about 3% that can be increased to 5% by treatment with chloronaphtalene and it can be obtained by a process whose synthetic complexity (SC)$_r$, defined in a recent report[2] by Po et al., is 45 on a scale 1-100. Our polymer **P**, synthesized by direct arylation, displayed similar maximum efficiency (around 3%) in untreated devices, but its synthetic complexity parameter drops to 40

(Table S1, Supporting Information), since the stannylation step of the donor comonomer is not required.

Results and Discussion

Synthesis of the random copolymer P. In principle, two polymerization routes (**a** and **b** in scheme 1) can be followed to obtain the ternary random copolymer **P** *via* DHAP.

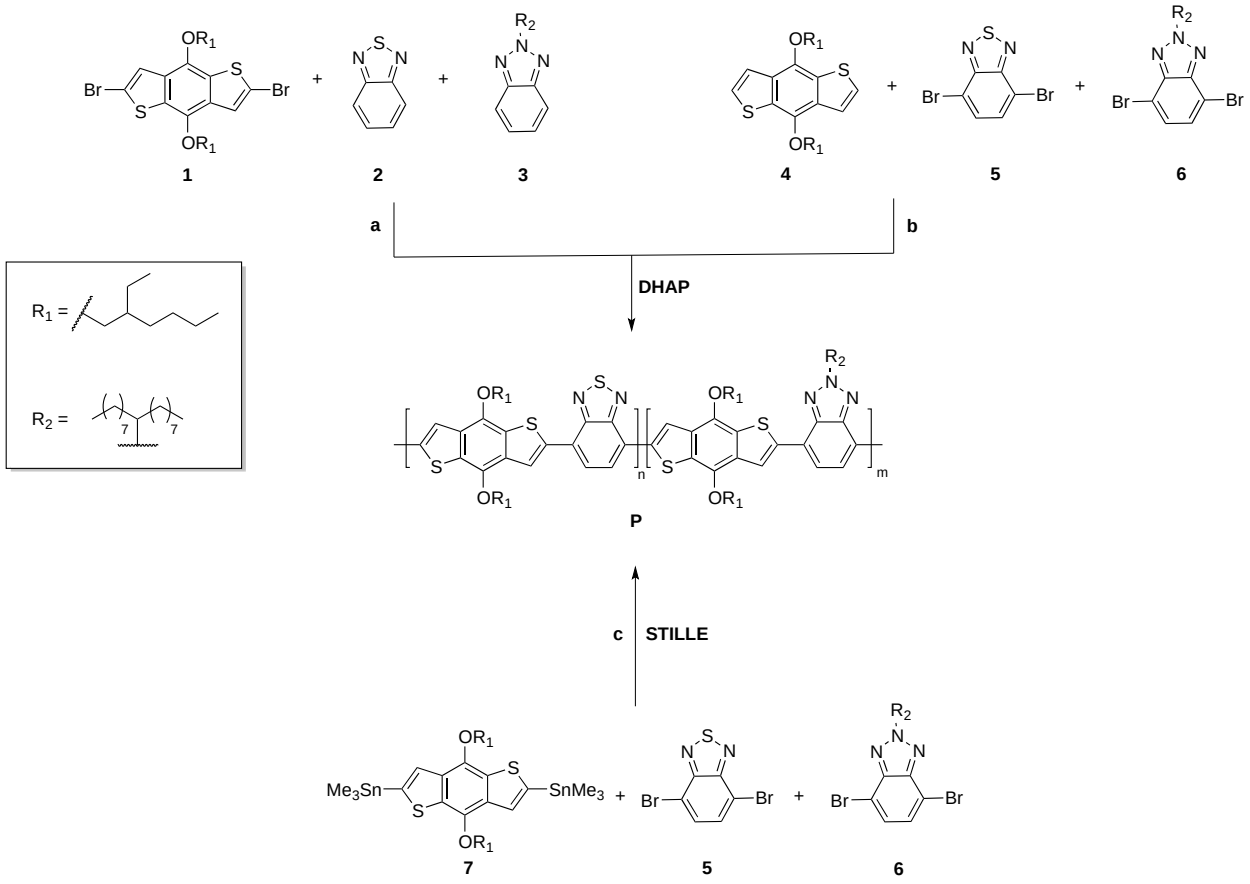

Scheme 1. DHAP (routes **a** and **b**) and Stille (route **c**) protocols for the synthesis of the copolymer **P**

Route **a**, carried out under the best conditions reported for DHAP of monomer **1** [Hermann-Beller catalyst (4% mol), pivalic acid (30% mol), P(o-MeOPh)$_3$ (8% mol), Cs_2CO_3 (2 equiv) in dry toluene for 36 hours],[23] failed to afford polymer **P**. This result can be likely ascribed to the

low acidity of the hydrogen atoms at the 4,7-positions of the electron-accepting units **2** and **3**, which do not easily undergo C-H bond activation step. Actually, it is well known that the heterolytic dissociation energy represents a critical factor influencing the regioselectivity of the direct arylation processes.[24] For this reason, the C-H bond ortho-functionalization with electron-withdrawing groups (e.g. fluorine atoms) is a common structural modification to increase the acidity of the hydrogen atoms thus enhancing the reactivity of the C-H bonds involved in the activation process.[25] Polymerization was thus performed *via* the route **b** by reacting benzodithiophene **4** with dibromobenzothiadiazole **5** and dibromobenzotriazole **6** in 2:1:1 ratio (Scheme 2). The process was investigated under various experimental conditions summarized in Table 1.

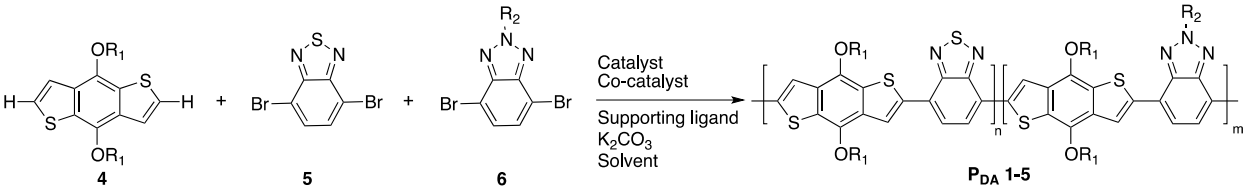

Scheme 2. General scheme of the DHAP

Table 1. Experimental conditions of the polymerization reactions and characterization of the polymers obtained.

Entry	**Polymer**	**Catalyst**	**Co-catalyst**	**Supporting ligand**	**Solvent**	**Temperature**	**Yield[a]**	**Molecular weight[b]** $M_w(M_n)$ **KDa**	λ_{max} **(nm)[c]**
Ref.[d]	$\mathbf{P_{STILLE}}$	$Pd(PPh_3)_4$ (1%mol)	/	/	Toluene	110°C	85%	61(20)	580
1	/	$Pd(OAc)_2$ (10%mol)	PivOH	/	NMP	120°C	/	/	

2	/	$Pd(OAc)_2$ (10%mol)	PivOH	/	NMP/ Toluene (1:1)	120°C	/	/	
3	/	$Pd(OAc)_2$ (10%mol)	PivOH	/	NMP, MW assisted	120°C	/	/	
4	/	$Pd(OAc)_2$ (10%mol)	PivOH	/	NBP	120°C	/	/	
5	**P_{DA}1**	$Pd(OAc)_2$ (10%mol)	PivOH	/	DMAc	120°C	50%	64 (9)	562
6	**P_{DA}2**	$Pd(OAc)_2$ (5%mol)	PivOH	/	DMAc	120°C	70%	73 (10.4)	551
7	**P_{DA}3**	$Pd(OAc)_2$ (5%mol)	PivOH	$PCy_3.HBF_4$	DMAc	120°C	70%	78 (10.3)	562
8	**P_{DA}4**	$Pd(OAc)_2$ (1%mol)	PivOH	/	DMAc	120°C	40%	18 (4.8)	564
9	**P_{DA}5**	$Pd_2(dba)_3$ (5%mol)	PivOH	$P(o\text{-}OMePh)_3$ (10%mol)	THF	Reflux	40%	14 (5.2)	578

[a] The products were obtained after Soxhlet extraction with hexane and by reprecipitation from $CHCl_3$/MeOH. [b] Estimated by GPC in trichlorobenzene (TCB) at 100°C calibrated on polystyrene standards. [c] Solid-state UV-Vis absorption maxima.[d] Reference reaction is a Stille polymerization according to ref. 22.

Different polar solvents were tested at 120°C in the presence of $Pd(OAc)_2$ (10% mol) as the pre-catalyst, pivalic acid (PivOH) as the carboxylate ligand and potassium carbonate as the base under phosphine-free conditions (Table 1, Entries 1-5).The reaction in *N,N*-dimethylacetamide (DMAc) afforded a polymer (M_w= 64 KDa, M_n= 9 KDa) in 50% yield. In *N*-methyl-pyrrolidinone (NMP), also with microwave assistance, the precipitation of a dark solid consisting of oligomeric products was observed during the polymerization. Only oligomers were also obtained in a mixture of NMP and Toluene (volumetric ratio 1:1) and in *N*-benzyl-pyrrolidinone (NBP) (used to increase the solubility of the products) (Entries 2 and 4).

Considering the positive outcomes of DHAP in DMAc, we further investigated the effects of other experimental conditions both on yields and molecular weights of the reaction carried out in this solvent.

Polymers with higher molecular weight were obtained in the presence of $Pd(OAc)_2$ 5% mol (Entries 5 and 6). Lowering the catalyst amount to 1% mol significantly reduced both the molecular weight and the yield of the final polymer. The use of tricyclohexylphosphine tetrafluoroborate ($PCy_3.HBF_4$) as a supporting ligand (Entry 7), which is known to have a marked positive effect on direct arylation processes,[26] did not afford significant change of molecular weight distribution and polydispersity index with respect to the phosphine-free reaction (Entry 6). This is an interesting result for the simplicity of the synthetic protocol and can positively affect the performances of the final material in the device. In fact, it is well known that inorganic impurities, if embedded in the polymer, can reduce the charge transport properties.[27-29] Lower molecular weight and yield (Table 1, Entry 9) were obtained by adopting different experimental conditions [$Pd_2(dba)_3$ and P(*o*-OMePh)$_3$ as catalyst and supporting phosphine ligand respectively in dry THF].[30]

Spectroscopic and optical characterization. The high-temperature ^{1}H NMR spectra of the polymer $\mathbf{P_{DA}2}$ and the reference $\mathbf{P_{STILLE}}$ in $C_2D_2Cl_4$ solution are compared in Figure 2.

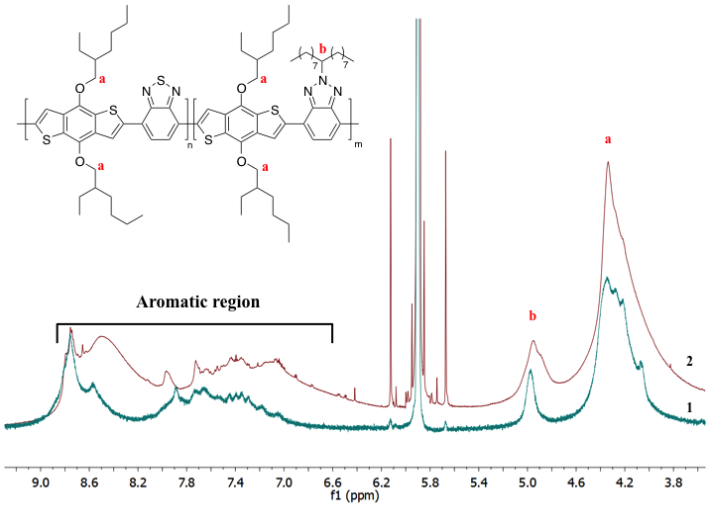

Figure 2. High temperature ^{1}H NMR spectra (400 MHz, $C_2D_2Cl_4$, 80°C) of polymers **P$_{DA}$2**(1) prepared by DHAP under the most favourable reaction conditions (Entry 6, Table 1) and **P$_{STILLE}$** (2) (Entry Ref., Table 1).

Comparison between the area values of the signal **b** at 4.98 ppm, related to the methine proton of the alkyl chain on the benzotriazole unit, and the broad signal **a** in the 4.50-3.93 ppm range, due to the OCH_2 protons of the alkyl chains on the benzodithiophene unit, enabled to assess that, in both the Stille and the DHAP reactions, the two accepting units (scheme 2) were incorporated into the polymer backbone in equimolecular amounts, according to the initial feed composition. Comparison of the aromatic regions of the spectra 1 and 2 clearly shows that there are some structural differences between the two polymers. These differences also appear in the UV-Vis absorption spectra of the polymers **P$_{DA}$1-P$_{DA}$5** *vs* **P$_{STILLE}$**. Thin film absorption spectra of **P$_{DA}$1-P$_{DA}$4** showed higher energy maxima with respect to the reference **P$_{STILLE}$** (Figure 3 and Table 1).

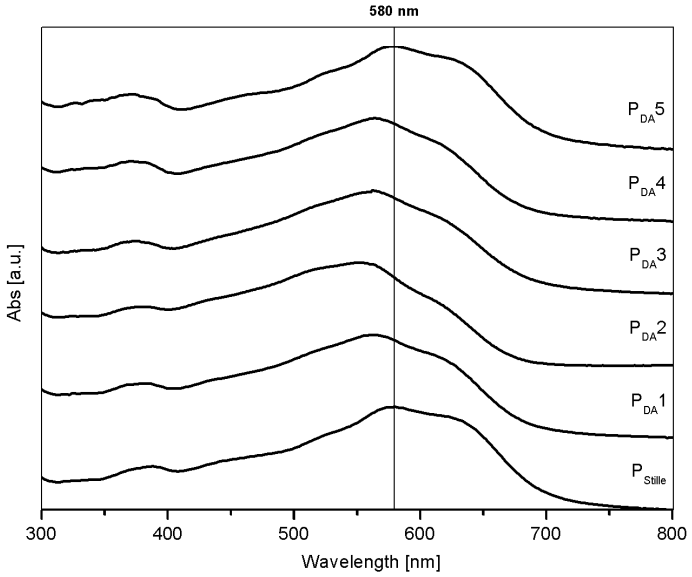

Figure 3. Normalized UV-Vis thin film absorption spectra of the polymers **P_{DA}1-P_{DA}5,** synthesized by DHAP, and **P_{STILLE}**, synthesized by Stille reaction.

This observation suggests that effective conjugation in **P_{DA}1-P_{DA}4** may be affected by structural defects. Only the spectrum of **P_{DA}5**, in spite of its lower molecular weight, closely resembles that of **P_{STILLE}**. This may suggest a more regular structure of **P_{DA}5** compared to **P_{DA}1-P_{DA}4** [although **P_{DA}5** performances in photovoltaic devices were markedly poor (see below)].

In DHAP, branching or cross-linking processes can occur during the reaction since both α and β C-H bonds of benzodithiophene could in principle be activated (Figure 4a), even if α-functionalization should be the most favourite process for stereo-electronic reasons.[24] On the contrary, in the Stille reaction (Figure 1, route **c**) the use of organotin reagent **7** fixes the regiochemistry of the coupling to the α-position of the benzodithiophene unit, ensuring a linear structure of the final polymer.

To gain insight into the regiochemical course of the DHAP in DMAc, we analyzed the reaction mixture during the first two hours of the polycondensation process. The polymerization reaction (Entry 6) was quenched after 1 hour or 2 hours and the main products were isolated out of the reaction mixtures by chromatography. We obtained five solid samples **F1**-**F5** (Chart 1) with increasing molecular weights and different colours, from yellow to purple, which suggest the growth of the chain length and π-conjugation as the reaction proceeds. After two hours, it was not possible to isolate single products because of the increased complexity of the reaction mixture.

Quenching the polymerization after 1h, the homocoupling product of benzodithiophene **F1** and the brominated coupling adduct of benzodithiophene and benzothiadiazole **F2** were isolated (Chart 1). After two hours, the main reaction products were **F3**, **F4**, and **F5**. The structures of these intermediates were completely assessed by high-resolution mass spectrometry and ^{1}H and ^{13}C NMR spectroscopy. The assignment of ^{1}H and ^{13}C NMR spectra required the use of both 1D and 2D techniques. The regiochemistry of the substitution at the benzodithiophene unit was studied by 2D NOESY experiments.

Quenching after 1h

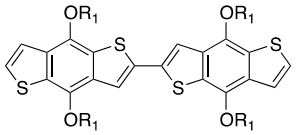

F1

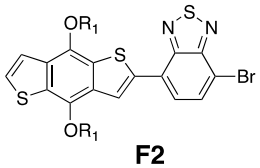

F2

Quenching after 2h

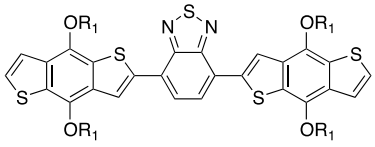

F3

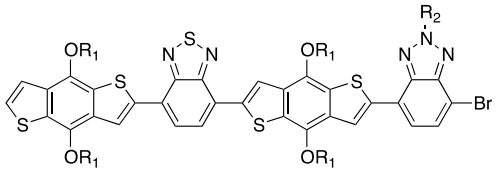

F4

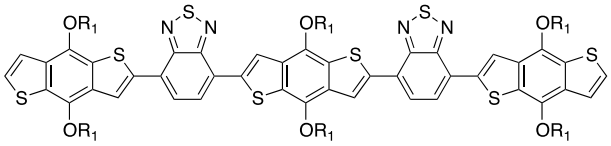

F5

Chart 1. Main products formed during the first two hours of DHAP in DMAc

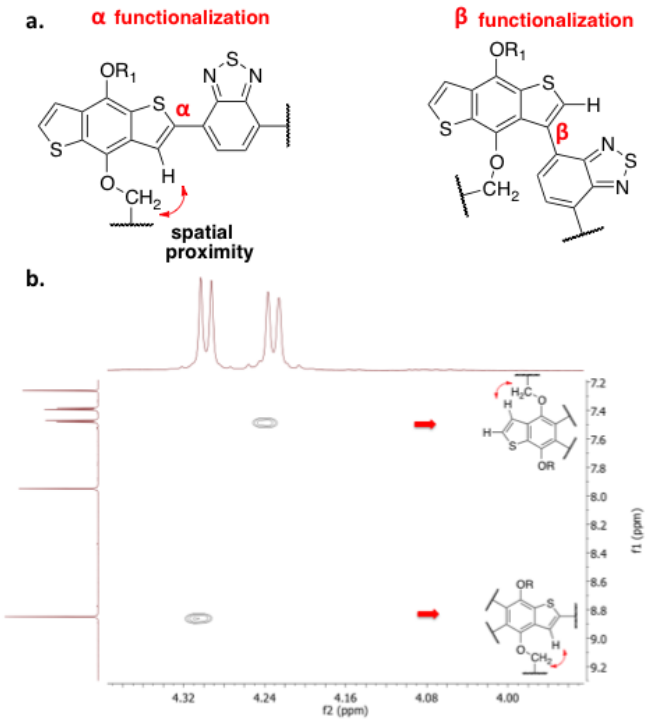

Figure 4. (a) α and β substitutions at the benzodithiophene unit. (b) Expansion of 500 MHz 2D NOESY spectrum of **F3**, acquired in $CDCl_3$, showing the cross region of OCH_2/thienyl protons of the benzodithiophene moiety.

As concerning **F1**, ^{1}H and ^{13}C NMR spectra were in close agreement with data already reported in the literature[31] and will be not further discussed. The structures of compounds **F2-F5** were elucidated considering some general features of their NMR spectra. Firstly, if mass spectrum indicates the presence of bromine in the molecule (also confirmed by a strongly shielded signal at nearly 110-115 ppm in the ^{13}C NMR spectra), there should be a benzothiadiazole or benzotriazole moiety as end unit of the molecule. Both benzotriazole and benzothiadiazole are characterized by similar ^{1}H and ^{13}C NMR aromatic resonances with chemical shift values strongly depending on substitution and degree of polymerization. Anyway, the inclusion of a benzotriazole unit in the oligomers is indicated by the typical ^{1}H and ^{13}C

resonances of the methine bonded to nitrogen (a ^{1}H septet at 4.9 ppm ca. and a ^{13}C resonance at 70 ppm ca.). For the benzodithiophene unit, the terminal thienyl moieties give rise to two doublets in the aromatic region with a typical vicinal coupling constant of about 5.5 Hz (chemical shifts are strongly influenced by the chemical environment), whereas substituted thienyl moieties give a strongly deshielded resonance in the region 8.5-9 ppm.

On the basis of these general considerations, the determination of the structure of **F2** was straightforward, since HR-MS confirmed the presence of a bromine atom, and the aromatic region of the ^{1}H NMR spectrum suggested the presence of a monosubstituted benzoditiophene unit (two doublets of an AX system at 7.41 and 7.48 ppm, respectively, with ^{3}J=5.5 Hz, and a singlet at 8.78 ppm) and a benzothiadiazole (two doublets at 7.76 and 7.89 ppm, respectively, with ^{3}J= 7.8 Hz).

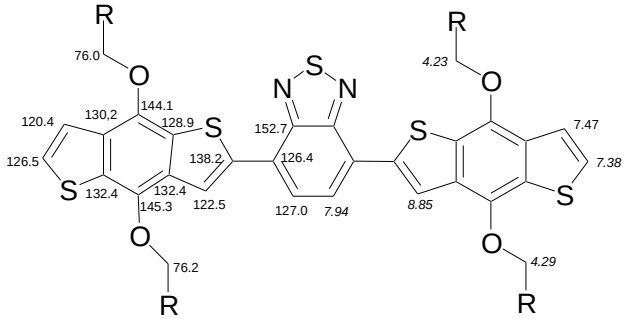

Figure 5. Chemical shifts (ppm) of ^{13}C and ^{1}H (italics) in oligomer **F3**

^{1}H and ^{13}C spectra of **F3** and **F5** indicated that (i) both molecules have symmetric structures (ii) the inclusion of benzotriazole units can be excluded and (iii) both compounds have two benzodithiophene end units. Moreover, the ^{1}H spectrum of **F3** consisted of only two doublets at 7.38 and 7.47 ppm, arising from the two equivalent thienyl moieties at both ends of the

molecule; one singlet at 8.85 ppm, due to the thienyl units bonded to benzothiadiazole; a singlet at 7.94 ppm arising from the two chemically equivalent benzothiadiazole protons. For **F5**, apart from the two doublets of terminal tiophenes at 7.08 and 7.22 ppm (^3J= 5.3 Hz) and an AB system centered at 7.45 ppm, which can be assigned to benzothiadiazole moieties, two singlets at 8.48 and 8.58 ppm suggested the existence of two chemically non-equivalent internal thienyl units.

For **F4**, ESI-MS indicated the presence of a bromine atom and hence a benzotriazole or benzothiadiazole end unit, whereas the ^{1}H NMR spectrum put in evidence that the molecule is not symmetric and is constituted by a terminal thienyl group (two doublets at 7.40 and 7.49 ppm with ^3J= 5.5 Hz), three non-equivalent internal thiophene rings, a benzotriazole and a benzothiadiazole unit (two doublets at 7.55 and 7.61 ppm with ^3J = 7.7 Hz and a more deshielded AB system centered at 8.00 ppm suggesting two protons with very similar shielding). The exact position of the benzotriazole and benzothiadiazole units was determined with the aid of HMBC and NOESYexperiments.

2D HSQC, HMBC and NOESY experiments were necessary to assign ^{1}H and ^{13}C NMR resonances (Table S2-S5, Supporting Information). The protonated carbons C-H were determined by HSQC experiments; HMBC and NOESY spectra allowed constructing the fragments in each molecule and their sequences. Only the aromatic regions and the characteristic signals of OCH_2 protons of the benzodithiophene units were taken into account. The aliphatic regions of both ^{1}H and ^{13}C the spectrum (alkyl chains on benzodithiophene and benzotriazole) are not of interest and were not considered. For all the compounds examined, the assignment of ^{1}H and ^{13}C NMR spectra (see Supporting Information) confirmed the structures in chart 1.

To determine the regiochemistry of the cross-coupling reaction, 2D NOESY spectra of **F3**-**F5** were acquired. Due to stereoelectronic factors, the α-arylation of the benzodithiophene ring by

C-H activation should be the most favourite process, but the β-attack cannot be excluded *a priori*. Considering the spatial arrangement of a benzodithiophene-benzothiadiazole (or benzotriazole, Figure 4a) fragment, if the thiophene ring is functionalized at the α-position, the β-hydrogen atom is in the close proximity to the O-CH_2- of one alkoxy chain on benzene ring. As a consequence, the through-space dipolar coupling between the thienyl proton and the methylene protons should give rise to a cross-correlation peak in the 2D NOESY spectrum. In the case of β-functionalization, no Overhauser effect between OCH_2 and thienyl proton can be observed. In the 2D NOESY spectrum of **F3,** a cross-peak between the methylene protons at 4.30 ppm and the internal thienyl proton at 8.85 ppm was well evident. Moreover, there was also a cross-peak between the other OCH_2 group at 4.23 ppm and the terminal thienyl proton at 7.47 ppm. Similar trends were observed also for the intermediates **F4** and **F5**.

In summary, these spectroscopic data indicate an initial regioregular evolution of the DHAP involving the α positions of the benzodithiophene units. Nevertheless, in advanced stages of the chains' growth, the number of the free β positions is markedly higher than the number of the α positions at the ends of the chains, and the β/α ratio increases as the reaction proceeds (Figure 6). For this reason, the formation of β defects in the polymer backbone may become statistically significant. This observation, together with the detected formation of homo-coupling defects **F1**, could rationalize the hypsochromic shift of the polymers synthesized by direct arylation in DMAc with respect to the reference **P**STILLE.

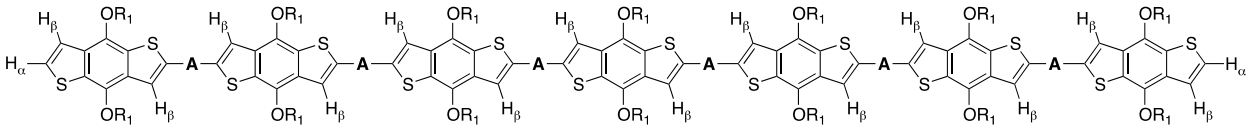

Figure 6. Alpha and beta positions on the thiophene rings during the chain growth.

Photovoltaic measurements. To explore **P_{DA}1-P_{DA}5** behaviour in solar cells, the polymers were blended with $PC_{71}BM$ (polymer: fullerene weight ratio 1:3). The device assembly and the preparation of blends were carried out using the experimental conditions reported for optimized solar cells based on **P_{STILLE}**.[22] The active layers (about 70 nm thick) were deposited on ITO/PEDOT-PSS from chlorobenzene (CB) solutions. Addition of a 2% (vol/vol) of 1-chloronaphthalene (CN) was reported to significantly improve the device performances (from 2.5% to 4%).[22] Ethanol surface treatment was carried out prior to evaporation of an aluminum cathode.

Table 2. Photovoltaic parameters of the polymers **P_{DA}1-P_{DA}5** and **P_{STILLE}** under different processing conditions.

Polymer: $PC_{71}BM$ (1:3)	Without CN processing				CN processing and ethanol surface treatment			
	V_{oc} [V]	FF [--]	J_{sc} [mA/cm^2]	PCE [a, b] [%]	V_{oc} [V]	FF [--]	J_{sc} [mA/cm^2]	PCE [a, b] [%]
P_{STILLE}	0.87	0.6	4.88	2.5	0.81	0.6	9.89	4.8
P_{DA}1	0.86	0.54	3.91	1.8	0.89	0.59	5.02	2.6
P_{DA}2	0.88	0.58	4.13	2.1	0.89	0.59	4.91	2.6
P_{DA}3	0.87	0.53	4.10	1.9	0.89	0.56	5.58	2.8
P_{DA}4	0.79	0.46	2.68	1.0	0.85	0.53	3.83	1.7

$P_{DA}5$	0.72	0.44	3.60	1.1	0.6	0.36	3.59	0.8

[a] Average PCE obtained from 6 devices [b] Standard deviations related to the PCE values are reported in Table S7 (Supporting Information)

As reported in Table 2, the photovoltaic parameters of **P_{STILLE}** are similar to **$P_{DA}1$- $P_{DA}3$** based devices, without CN processing. When the active layer is deposited from CB, the J_{sc} is 4.8 mA/cm^2 for **P_{STILLE}** and ranges from 3.9 to 4.1 mA/cm^2 for the **$P_{DA}1$- $P_{DA}3$** based devices (Table 2). CN processing induces an almost 2-fold enhancement to 9.8 mA/cm^2 for **P_{STILLE}** while the J_{sc} of **P_{DA}-s** is not significantly improved by this treatment, with J_{sc} values ranging from 4.9 to 5.6 mA/cm^2. The observed enhancement of J_{sc} with CN processing is due to a reduction of phase segregation and a better degree of intermixing between the donor polymer and the acceptor fullerene that induces an enhancement of charge photogeneration.[22, 32] Small improvements of the photovoltaic performances were also obtained with ethanol surface treatment. This treatment does not substantially affect the blend morphology (see Supporting Information) but it likely reduces the barrier at the electrodes/active layer interface.[33]

Upon CN processing and ethanol surface treatment the PCE for all polymers obtained by DHAP is lower than that of P_{STILLE} (Table 2). Interestingly, the PCE decreases with the polymer molecular weight. This decrease is consistent with previous studies reported in the literature, which suggested that, below Mn≈10000 g/mol, the photovoltaic properties of polymer based BHJ solar cells are affected, by non optimal blend morphologies and poor opto-electronic properties.[34-36]

It can be seen from Table 2 that, in devices obtained with CN processing and ethanol surface treatment, there is a substantial drop of J_{sc} going from **P_{STILLE}** to **$P_{DA}1$-$P_{DA}5$**, which is quite significant in **$P_{DA}4$** and **$P_{DA}5$**. The active layers were analysed by optical microscopy to check

whether such behaviour is related to differences in the film forming properties. Figure 7 shows the typical images obtained for the active layers. The aspect of **P_{DA}1-P_{DA}3** films is similar to **P_{STILLE}** active layer, while **P_{DA}4** and **P_{DA}5** active films exhibit a strong segregation at the microscopic scale. Furthermore, a strong scattering background is observed for **P_{DA}5** blends (Supporting Information). These features can explain the lower photovoltaic performances of **P_{DA}4** and the even poorer characteristics of **P_{DA}5** based devices.

P_{STILLE}:$PC_{71}BM$ (1:3 w:w)	**P_{DA}2:$PC_{71}BM$ (1:3 w:w)**	**P_{DA}4:$PC_{71}BM$ (1:3 w:w)**
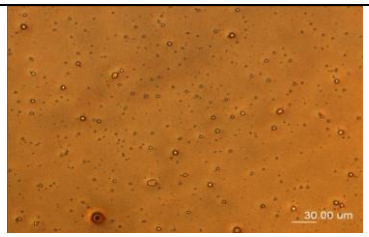	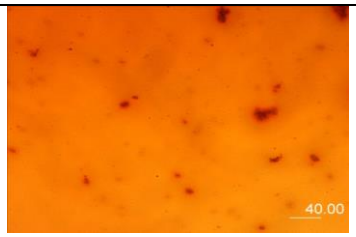	

Figure 7. Optical photography of the 1:3 **P_{STILLE}**: $PC_{71}BM$ and **P_{DA}-s**:$PC_{71}BM$ blends deposited from CB+2%CN

Further support to this hypothesis derives from a deep AFM microscopy analysis of the **P_{STILLE}** and **P_{DA}1-P_{DA}3** blends. Figure 8 compares the AFM morphologies of **P_{STILLE}** and **P_{DA}2** through the CN processing. It can be seen that an extended phase segregation, with similar large domains, is observed in the blends deposited from CB. This feature is consistent with the similar J_{sc} parameters obtained prior to CN processing. It is also evident a significant reduction of phase segregation upon CN addition. **P_{STILLE}** based film exhibits a more intermixed morphology when compared to **P_{DA}2**. This is consistent with the more pronounced improvement of J_{sc} observed in **P_{STILLE}** than in **P_{DA}1-P_{DA}3** devices upon processing.

P_{STILLE}:$PC_{71}BM$ (1:3 w:w) CB	$P_{DA}2$:$PC_{71}BM$ (1:3 w:w), CB
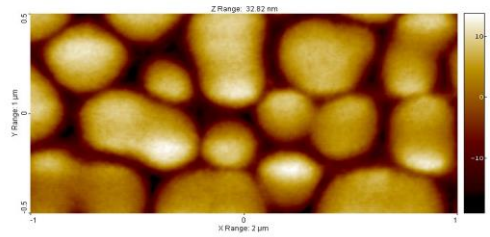	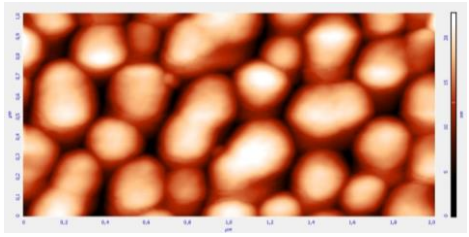
P_{STILLE}:$PC_{71}BM$ (1:3 w:w) CB+CN	**$P_{DA}2$:$PC_{71}BM$ (1:3 w:w),CB+CN**
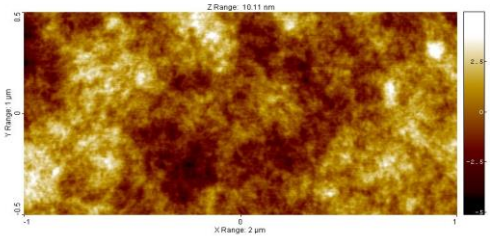	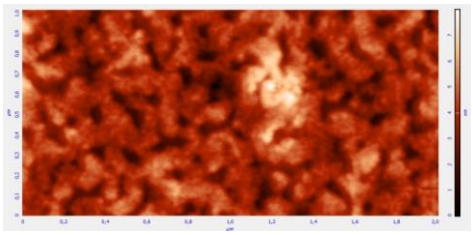

Figure 8. AFM images (2 μm x 1 μm) of the 1:3 **P_{STILLE}**: $PC_{71}BM$ and **$P_{DA}2$**:$PC_{71}BM$ blends deposited from CB (upper row) and CB+2% CN (lower row)

Conclusions. An example of three-component random polymerization *via* DHAP involving two different accepting units has been reported for the first time. The experimental results are discussed in comparison with the properties of the same copolymer obtained *via* the Stille reaction. The regiochemical course of the reaction in the early stage of the polymerization process has been investigated by NMR spectroscopy. Photovoltaic parameters for the synthesized polymers have been evaluated in comparison with **P_{STILLE}**. **P_{STILLE}** showed similar power conversion efficiencies to **P_{DA}** in devices without processing with chloronaphtalene. CN processing strongly increases the performances of **P_{STILLE}** while **P_{DA}** polymers are almost

insensitive to this treatment. This trend can reasonably be ascribed to the lower molecular weights (M_n) and/or structural defects of DHAP polymers.

We consider DHAP as a valid protocol for the synthesis of active materials, alternative to conventional cross-coupling reactions (e.g Stille, Suzuki), also in view of a possible scalability at industrial level. In fact, an estimate of the reduced synthetic complexity parameter from 45 to 40 is calculated switching from Stille to DHAP reaction. Random polymerizations *via* DHAP involving synthetically simple monomers could represent a promising approach, which undoubtedly deserves more investigation.

Experimental section

Materials. 2,6-dibromo-4,8-bis((2-ethylhexyl)oxy)benzo[1,2-b;4,5-b']dithiophene **1**, 4,8-bis((2-ethylhexyl)oxy)benzo[1,2-b; 4,5-b']dithiophene **4**, Hermann-Beller catalyst,4,7-dibromo-2-(heptadecan-9-yl)-2H-benzo[d][1,2,3]triazole **6** were purchased from Sunatech Inc. and used without further purification. The compounds benzo[c][1,2,5]thiadiazole **2**, pivalic acid, potassium carbonate, cesium carbonate, palladium (II) acetate, tris(dibenzylideneacetone)dipalladium(0),tris(o-methoxyphenyl)phosphine, ammonium hydroxide solution, N-methyl-pyrrolidinone, N-benzyl-pyrrolidinone, methanol, acetone and chloroform were purchased from Sigma Aldrich and used without further purification.4,7-dibromobenzo[c][1,2,5]thiadiazole **5** was purchased from Sigma Aldrich and recrystallized from ethyl acetate. Tricyclohexylphosphine tetrafluoborate was purchased from TCI. 2-(heptadecan-9-yl)-2H-benzo[d][1,2,3]triazole **3** was prepared according to the reported procedure.[22] N,N-dimethylacetamide was purchased from Sigma Aldrich and degassed before use. THF and

Toluene were distilled from sodium with benzophenone as an indicator under nitrogen atmosphere. Polymer **P_{DA}5** was prepared according to a reported procedure.[30]

Typical procedure for the synthesis of the copolymer P_{DA}2 *via* DHAP. In a three-necked round-bottomed flask (25 mL), monomer **4** (458 mg, 1.02 mmol), monomer **5** (151 mg, 0.51 mmol), monomer **6** (263 mg, 0.51 mmol), potassium carbonate (354 mg, 2.56 mmol) and pivalic acid (32 mg, 0.31 mmol) were dissolved in degassed N,N-dimethylacetamide(12 mL) under nitrogen atmosphere. $Pd(OAc)_2$ (6 mg, 0.025 mmol) was added and the reaction mixture was heated at 120° for 48 hours. After this time, the polymer was end-capped by adding monomer **4** (2.3 g, 5.13 mmol). The whole mixture was cooled to room temperature and poured in methanol. The solid product was washed with water, recovered by filtration and purified by Soxhlet extraction using methanol, acetone and hexane, respectively. The solid residue was dissolved in chloroform (5 mg/mL) and an aqueous ammonia solution (NH_4OH) was added (volumetric ratio= 1:1). The mixture was refluxed for 5 hours under vigorous stirring and then it was cooled to room temperature. The organic phase was separated, concentrated and the polymer re-precipitated from methanol. A dark purple solid was recovered by filtration and dried under vacuum at 60°C to yield the target polymer (501 mg, yield = 70%).

P_{DA}2. ^{1}H NMR ($C_2D_2Cl_4$, 500 MHz, 80°C): δ_H 9.07-8.24 (4H, br), 8.11-6.88 (5H, br), 5.11-4.81 (1H, br), 4.56-3.81 (11H, br), 2.48-0.38 (160H, br). GPC (TCB, 100°C, polystyrene standards): M_w = 73 KDa, M_n= 10.4KDa. UV-Vis ($CHCl_3$, λ_{max}) 540 nm. UV-Vis (thin film, λ_{max}) 551 nm.

Procedure for the isolation of the main coupling products in the early stage of the polycondensation. Two polymerization reactions, performed as described in the previous

procedure, were quenched after 1hour and 2 hours, respectively, by adding water to the reaction mixture. Then, the mixture was poured in a separatory funnel and extracted by dichloromethane for three times. The organic phases were separated, dried over anhydrous sodium sulphate and filtered under vacuum. After the evaporation of the solvent, the crude products were purified by silica column chromatography under gradient elution (from hexane: dichloromethane = 9:1 to hexane: dichloromethane = 6:4) to give fragments **F1**-**F5** (Chart 1).

F1. Spectroscopic data are in agreement with the data reported in the literature. [31]

F2. ^{1}H NMR ($CDCl_3$, 500 MHz): δ_H 8.78 (1H, s), 7.89 (1H,d, *J*= 7.7 Hz), 7.76 (1H, d, *J*= 7.7 Hz), 7.48 (1H, d, *J*= 5.5 Hz), 7.41 (1H, d, *J*= 5.5 Hz), 4.27 (2H, d, *J*= 5.3 Hz), 4.21 (2H, dd, *J*= 5.4 Hz, *J*=0.9 Hz), 1.89-1.58 (10H, m), 1.51-1.36 (8H, m), 1.07 (3H, t, *J*= 7.4 Hz), 1.04 (3H, t, *J*= 7.4 Hz), 0.98-0.93 (6H, m). ^{13}C{^{1}H} NMR ($CDCl_3$, 100 MHz): δ_C 153.8, 151.8, 145.3, 144.1, 137.4, 132.5, 132.2, 132.1, 130.3, 128.8, 127.1, 127.0, 126.5, 122.8, 120.3, 113,3, 76.2, 76.1, 40.78, 40.75, 30.7, 30.5, 29.8, 29.4, 29.3, 24.02, 23.96, 23.3, 23.2, 14.3, 11.6, 11.5. HR-MS: pred. value for $[M]^+$ of $C_{32}H_{39}N_2O_2S_3Br$, 658.1352, meas. 658.1333.

F3. ^{1}H NMR ($CDCl_3$, 500 MHz): δ_H 8.85 (1H, s), 7.94 (1H, s), 7.47 (1H, d, *J*= 5.5 Hz), 7.38 (1H, d, *J*= 5.5 Hz), 4.29 (2H, d, *J*= 5.1 Hz), 4.23 (2H, d, *J*= 5.3 Hz), 1.94-1.59 (10H, m), 1.54-1.36 (10H, m), 1.10 (3H, t, *J*= 7.4 Hz), 1.06 (3H, t, *J*= 7.2 Hz), 1.02-0.94 (6H, m).^{13}C{^{1}H}NMR ($CDCl_3$, 100 MHz): δ_C152.7, 145.3, 144.1, 138.2, 132.4, 130.2, 128.9, 127.0, 126.5, 126.4, 122.5, 120.4, 76.2, 76.0, 40.8, 30.7, 30.5, 29.8, 29.4, 29.3, 24.0, 23.3, 14.3, 11.6, 11.5. HR-MS: pred. value for $[M]^-$ of $C_{58}H_{76}N_2O_4S_4$, 1024.4414, meas. 1024.4330.

F4. ^{1}H NMR ($CDCl_3$, 500 MHz): δ_H 8.87 (1H, s), 8.85 (1H, s), 8.72 (1H, s), 8.00 (1H, d, *J*= 7.7 Hz), 7.98 (1H, d, *J*= 7.7 Hz), 7.61 (1H, d, *J*= 7.7 Hz), 7.55 (1H, d, *J*= 7.7 Hz), 7.49 (1H, d, *J*= 5.5 Hz), 7.40 (1H, d, *J*= 5.5 Hz), 4.94 (1H, septet, *J*= 4.7 Hz), 4.41-4.32 (4H, m), 4.30 (2H, d, *J*= 5.2

Hz), 4.24 (2H,d, *J*= 5.5 Hz), 2.32-2.22 (4H, m), 2.08-1.98 (4H, m), 1.97-1.57 (20H, m), 1.54-1.38 (16H, m), 1.24-1.16 (18H, m), 1.13 (3H, t, *J*= 7.5 Hz), 1.11 (3H, t, *J*= 7.5 Hz), 1.10 (3H, t, *J*= 7.4 Hz), 1.06 (3H, t, *J*= 7.5 Hz), 1.02-0.94 (9H, m), 0.91-0.86 (3H, m), 0.85-0.79 (6H, m).$^{13}C\{^{1}H\}$NMR ($CDCl_3$, 100 MHz): δ_C 152.85, 152.84, 145.4, 144.9, 144.8, 144.2, 143.7, 141.6, 138.74, 138.68, 138.3, 133.3, 133.2, 132.51, 132.49, 130.4, 129.3, 129.2, 129.0, 128.9, 127.2, 127.1, 126.7, 126.6, 124.4, 124.3, 122.60, 122.58, 122.0, 120.4, 110.3, 76.3, 76.2, 76.1, 69.2, 40.79, 40.76, 40.70, 35.7, 31.9, 31.8, 30.7, 30.6, 30.5, 29.70, 29.66, 29.4, 29.35, 29.33, 29.31, 29.25, 29.19, 29.16, 26.1, 24.03, 23.99, 23.97, 23.9, 23.3, 23.23, 23.18, 22.7, 22.6, 14.28, 14.26, 14.23, 14.22, 14.19, 14.1, 14.0, 11.53, 11.52, 11.5, 11.4. HR-MS: pred. value for $[M]^-$ of $C_{81}H_{112}N_5O_4S_5Br$, 1457.6507, meas. 1457.6368.

F5. ^{1}H NMR ($CDCl_3$, 500 MHz): δ_H 8.58 (2H, s), 8.47 (2H, s), 7.44 (4H, AB system, *J*≅ 7Hz), 7.22 (2H, d, *J*= 5.3 Hz), 7.08 (2H, d, *J*= 5.3 Hz), 4.22-4.07 (12H, m), 1.95-1.39 (54H, m), 1.23 (6H, t, *J*= 7.2 Hz), 1,14 (6H, t, *J*= 7.4 Hz), 1.11 (6H, t, *J*= 6.9 Hz), 1.1 (6H, t, *J*= 7.4 Hz), 1.06-1.00 (12H, m). $^{13}C\{^{1}H\}$ NMR ($CDCl_3$, 100 MHz): δ_C 152.2, 144.9, 144.2, 143.8, 138.4, 138.2, 133.0, 132.3, 132.0, 129.9, 128.8, 128.6, 126.3, 126.1, 126.0, 125.6, 122.2, 120.1, 75.7, 75.6, 75.4, 40.9, 40.8, 40.7, 30.8, 30.7, 30.5, 29.5, 29.4, 29.3, 24.1, 24.0, 23.9, 23.4, 23.3, 23.2, 14.5, 14.4, 14.3, 11.7, 11.6, 11.5. HR-MS: pred. value for $[M+H]^+$ of $C_{90}H_{114}N_4O_6S_8$, 1603.6643, meas. 1603.6567.

Measurement and Instruments. ^{13}C NMR spectra were acquired on a Varian INOVA 400 spectrometer at 100.61 MHz and ^{1}H NMR spectra were acquired on a Varian INOVA500 spectrometers at 500.13 MHz. Samples **F1-F5** were dissolved in $CDCl_3$ and the spectra were acquired at room temperature. The chemical shifts of ^{1}H and ^{13}C were reported relative to the residual chloroform signals at 7.26 and 77 ppm, respectively. Poorly soluble polymers $\mathbf{P_{Stille}}$ and

P$_{DA}$2 were dissolved in $C_2D_2Cl_4$ (residual signal at 5.90 ppm) and the spectra were acquired at 80°C. High-resolution mass spectra were acquired on a SHIMADZU high performance liquid chromatography-ion trap-time of flight mass spectrometer (LCMS-IT-TOF) *via* direct infusion of the samples using chloroform as the solvent. Gel permeation chromatography (GPC) analyses were performed with a Agilent 220 chromatograph equipped with a refractive index detector on 1,2,4-trichlorobenzene (TCB) solutions at 80°C in order to overcome aggregation phenomena. Molecular weight calibration was carried out using polystyrene standards. UV-Vis spectra of the polymers were recorded on SHIMADZU UV-2401PC. Optical images were collected using with a Nikon Eclipse TE2000-U inverted confocal microscope. Atomic force microscopy (AFM) investigations were performed using a NT-MDTNTEGRA apparatus in tapping mode under ambient conditions.

Device fabrication. All polymers, synthesized using DHAP method, were investigated in bulk heterojunction PV devices with a typical sandwich structure glass/ITO/PEDOT:PSS/active layer/Al. The sample preparation was carried out according to a procedure previously described.[22] On the basis of this procedure, 1:3 weight ratio of copolymer: $PC_{71}BM$ was selected for all tested new polymers. The active layers were prepared from chlorobenzene solution with 1-chloronaphtalene as additive. As for optimized **P$_{STILLE}$**, all the active films based on the new copolymers investigated were surface treated with ethanol prior to the cathode deposition. To finish the device fabrication, 100 nm aluminum were thermally evaporated on the active layer.

ASSOCIATED CONTENT

Supporting Information.

Synthetic complexity (SC) table of the copolymer P, spectroscopic and optical characterization of oligomers F2-F5, device characterization. This material is available free of charge via the Internet at http://pubs.acs.org.

AUTHOR INFORMATION

Corresponding Author

Prof. Gianluca Maria Farinola

Dipartimento di Chimica, Università degli Studi di Bari Aldo Moro,

Via Orabona 4, 70125, Italy

Fax: +39-0805442064

E-mail: gianlucamaria.farinola@uniba.it

Author Contributions

The manuscript was written through contributions of all authors. All authors have given approval to the final version of the manuscript

Funding Sources

Ministero dell'Istruzione, dell'Università e della Ricerca; Università degli Studi di Bari Aldo Moro:

1. Progetto PRIN2012 prot. 2012A4Z2RY "Aqueous Processable Polymer Solar Cells: from Materials to Photovoltaic Modules" (AQUA-SOL)

2. Progetto PON 02_00563_3316357 "Nanotecnologie Molecolari per la Salute dell'Uomo e l'Ambiente_MAAT"

ACKNOWLEDGMENT

MIUR with Università degli Studi di Bari Aldo Moro (Progetto PRIN2012 prot. 2012A4Z2RY and Progetto PON 02_00563_3316357 "Nanotecnologie Molecolari per la Salute dell'Uomo e l'Ambiente_MAAT"); Regione Puglia (APQ Reti di Laboratorio "Laboratorio Regionale di Sintesi e Caratterizzazione di Nuovi Materiali Organici e Nanostrutturati per Elettronica, Fotonica e Tecnologie Avanzate" Prog. Cod. 20) and Eni SpA are acknowledged for the financial support.

REFERENCES

(1) Marzano, G.; Ciasca, C.V.; Babudri, F.; Bianchi, G.; Pellegrino, A.; Po, R.; Farinola, G.M. *Eur. J. Org. Chem* **2014**, *30*, 6583-6614.

(2) Po, R.; Bianchi, G.; Carbonera, C.; Pellegrino, A. *Macromolecules* **2015**, *48*, 453-461.

(3) You, J.; Dou, L. ; Yoshimura, K. ; Kato, T. ; Ohya, K. ; Moriarty, T. ; Emery, K. ; Chen, C-C.; Gao, J.; Li, G.; Yang, Y. *Nat. Commun.* **2013**, *4*, 1446

(4) Liu, Y.; Zhao, J.; Li, Z.; Mu, C.; Ma, W.; Hu, H.; Jiang, K. ; Lin, H. ; Ade, H. ; Yan, H. *Nat. Commun.* **2014**, *5*, 5293.

(5) Cheng, Y-J. ; Yang, S-H. ; Hsu, C-S. *Chem. Rev.* **2009**, *109*, 5868-5923.

(6) Liao, S.-H. ; Jhuo, H.-J. ; Cheng, Y.-S. ; Chen , S.-A. *Adv. Mater.* **2013**, *25*, 4766-4771.

(7) He, Z.; Zhong, C.; Su, S.; Xu, M.; Wu, H.; Cao, Y. *Nat. Photon.* **2012**, *6*, 591-595.

(8) Guo, X.; Zhou, N.; Lou, S. J.; Smith , J.; Tice, D. B.; Hennek, J. W.; Ponce Ortiz, R.; Lòpez Navarrete, J. T.; Li, S.; Strzalka, J.; Chen, L. X.; Chang, R. P. H.; Facchetti, A.; Marks, T. J. *Nat. Photon.* **2013**, *7*, 825-833.

(9) Lu, L.; Xu,T.; Chen, W.; Lee, J.; Luo, Z.; Jung, I.; Kim S.; Yu, L. *Nano Lett.* **2013**, *13*, 2365−2369.

(10) Mercier, G.L. ; Leclerc, M. *Acc. Chem. Res.* **2013**, *46*, 1597−1605.

(11) Grenier, F.; Aich, B.R.; Lai, Y.Y.; Guerette, M.; Holmes, A.B.; Tao, Y.; Wong, W.W.H.; Leclerc, M. *Chem. Mater.* **2015**, *27*, 2137−2143.

(12) Allard, N.; Zindy, N., Morin, P.O.; Wienk, M.M.; Janssen, R.A.J.; Leclerc, M. *Polym. Chem.* **2015**, *6*, 3956-3961.

(13) Iizuka, E.; Wakioka, M.; Ozawa, F. *Macromolecules* **2015**, *48*, 2989-2993.

(14) Wakioka, M., Ichihara, N.; Kitano, Y.; Ozawa, F. *Macromolecules* **2014**, *47*, 626-631.

(15) Morin, P.-O., Bura, T.; Sun, B.; Gorelsky, S.I.; Li, Y.; Leclerc, M. *ACS Macro Lett.* **2015**, *4,* 21-24.

(16) Okamoto, K.; Zhang, J.; Housekeeper, J.B. ; Marder, S.R. ; Luscombe, C.K. *Macromolecules* **2013**, *46*, 8059−8078.

(17) Kuwabara, J.; Yasuda, T.; Choi, S.J. ; Lu, W. ; Yamazaki, K.; Kagaya, S.; Han, L.; Kanbara, T. *Adv. Funct. Mater.* **2014**, *24*, 3226-3233.

(18) Rudenko, A.E. ; Thompson, B.C. *J. Polym. Sci. Pol. Chem.* **2015**, *53*, 135−147.

(19) Kang, T.E.; Kim, K.-H., Kim B. *J. Mater. Chem. A* **2014**, *2*, 15252−15267.

(20) Woo, C.H. ; Thompson, B.C. ; Kim, B.J. ; Toney, M.F.; Frechet J.M.J. *J. Am. Chem. Soc.* **2008**, *130*, 16324−16329.

(21) Rudenko, A.E. ; Wiley, C.A. ; Stone, S.M. ; Tannaci, J.F. ; Thompson, B.C. *J. Polym. Sci. Pol. Chem.* **2012**, *50*, 3691−3697.

(22) Kotowski, D.; Luzzati, S. ; Bianchi, G.; Calabrese, A.; Pellegrino, A.; Po, R.; Schimperna, G.; Tacca, A. *J. Mater. Chem* **2013**, *1*, 10736-10744.

(23) Beauprè, S.; Pron, A.; Drouin, S.H. ; Najari, A.; Mercier, L.G. ; Robitaille, A.; Leclerc, M. *Macromolecules* **2012**, *45*, 6906-6914.

(24) Gorelsky, S. I. *Coord. Chem. Rev.* **2013**, *257*, 153-164.

(25) Lu, W.; Kuwabara, J. ; Iijima, T. ; Higashimura, H.; Hayashi, H. ; Kanbara, T. *Macromolecules* **2012**, *45*, 4128-4133.

(26) Campeau, L.-C. ; Fagnou, K. *Chem. Commun.* **2006**, 1253-1264.

(27) Camaioni, N.; Tinti, F. ; Franco, L. ; Fabris, M.; Toffoletti, A. ; Ruzzi, M. ; Montanari, L. ; Bonoldi, L. ; Pellegrino, A. ; Calabrese, A. ; Po, R. *Organic Electronics* **2012**, *13*, 550-559.

(28) Nikiforov, M.P.; Lai, B.; Chen, W.; Chen, S.; Schaller, R.D.; Strzalka J.; Maser, J.; Darling, S.B. *Energy Environ. Sci.* **2013**, *6*, 1513-1520.

(29) Troshin, P.A.; Susarova, D.K.; Moskvin, Y.L.; Kuznetsov, I.E.; Ponomarenko, S.A.; Myshkovskaya, E.N.; Zakharcheva, K.A.;Balakai, A.A.; Babenko, S.D.; Razumov, V.F. *Adv. Funct. Mater.* **2010**, *20*, 4351-4357.

(30) Wang, X.; Wang, X. *Polym. Chem.* **2014**, *5*, 5784-5792.

(31) Braunecker, W.A.; Oosterhout, S.D.; Owczarczyk, Z.R.; Kopidakis, N.; Ratcliff, E.L.; Ginley, D.S.; Olson, D.C. *ACS Macro Lett.* **2014**, *3*, 622-627.

(32) Hoven, C.V; Dang, X.-D.; Coffin, R.C.; Peet, J.; Nguyen, T.-Q.; Bazan, G.C. *Adv. Ener. Mater.* **2010**, *22*, E63–E66.

(33) Liu, X.; Wen, W.; Bazan, G.C. *Adv. Mater.* **2012**, *24*, 4505-4510.

(34) Muller, C.; Wang, E.; Andersson, L.M.; Tvingstedt, K.; Zhou, Y.; Andersson, M.R.; Inganas O. *Adv. Funct. Mater.* **2010**, *20*, 2124-2131.

(35) Schilinsky, P.; Asawapirom, U.; Scherf, U.; Biele, M.; Brabec, C.J. *Chem. Mater*. **2005**, *17*, 2175-2180.

(36) Tong, M.; Cho, S.; Rogers, J.T.; Schmidt, K.; Hsu, B.B.Y.; Moses, D.; Coffin, R.C.; Kramer, E.J.; Bazan G.C.; Heeger, A.J. *Adv. Funct. Mater*. **2010**, *20*, 3959-3965.